JOURNAL OF AGRICULTURAL AND FOOD CHEMISTRY

pubs.acs.org/JAFC Article

Chronic Exposure to Sunset Yellow Promotes Susceptibility to Experimental Colitis in Mice through Gut Microbiota

Xinyi Shi, Li Wan, Shanhong Ni, Xin Wu, Jing Mu, Wenlong Pei, Zeyuan Chen, Yu Xia, Lei Li, and Zhan Zhang*

Cite This: J. Agric. Food Chem. 2025, 73, 23633−23643 Read Online

ACCESS | Metrics & More | Article Recommendations | Supporting Information

ABSTRACT: Sunset yellow (SY) is a widely used food additive. However, its impacts on ulcerative colitis (UC) development remain unclear. Here, SY exposure exacerbated dextran sulfate sodium (DSS)-induced UC symptoms in mice, including body weight loss, elevated disease activity index, histological damage, inflammation, gut barrier impairment, disruption of gut microbiota composition, and sulfur metabolism. Moreover, fecal microbiota transplantation from SY-exposed mice also exacerbated colitis in the recipient mice. Notably, SY exposure both *in vivo* and *in vitro* inhibited the growth of *Akkermansia muciniphila* (*AKK*). Nontargeted metabolomics revealed that SY exposure impaired glutathione (GSH) metabolism, as evidenced by reduced GSH and glutathione disulfide levels in both normal and colitis mice. In *AKK*, SY exposure significantly decreased GSH content, suppressed glutathione S-transferase activity, and disrupted sulfur metabolism. Importantly, GSH supplementation markedly reversed the SY-induced *AKK* growth inhibition. Collectively, these findings suggest that long-term SY exposure promotes experimental colitis in mice through gut microbiota-dependent GSH metabolic dysregulation.

KEYWORDS: *food additives, ulcerative colitis, glutathione, oxidative stress, gut microbiota, metabolome, transcriptome*

INTRODUCTION

Ulcerative colitis (UC) is a type of inflammatory bowel disease (IBD), similar to Crohn's disease (CD). UC can significantly impact patients' quality of life and may lead to serious complications. Long-term UC can result in structural and functional changes in the colon, increasing the risk of colorectal cancer.[1,2] The incidence of IBD is highest in Western countries, with rates ranging from 10 to 30 per 100,000 people.[3] As the incidence of UC continues to rise globally, the overall disease burden is expected to increase due to its relatively low mortality rates.[4] Although genetic predisposition, disturbances in gut microbiota, and environmental factors are known contributors to IBD onset,[5,6] the exact pathogenesis remains unclear. There is increasing evidence that diet plays a key role in the development of IBD.[7,8]

Food additives such as emulsifiers, sweeteners, and synthetic colorants are widely used to improve the texture, taste, and color of processed foods. Although food additives are generally recognized as safe, emerging evidence suggests their potential adverse health effects, including dysbiosis, increased intestinal permeability, and inflammation.[9] Higher intake of emulsifier was positively correlated with serum inflammatory biomarker glycoprotein acetyls.[10] Compared with healthy controls, CD patients in Australia and China consumed more food additives, including total emulsifiers, sweeteners, and titanium dioxide (TiO_2) nanoparticles, in the past year.[11] Polysorbate 80 and sucralose decreased butyrate-producing bacteria, while increased bacterial species positively correlated with intestinal inflammation and fibrosis, especially in donors in remission of IBD.[12] TiO_2, commonly used as a whitener or brightener, exacerbated DSS-induced colitis by disrupting intestinal barrier function and activating the inflammasome.[13] Previous studies revealed that chronic exposure to Allura Red, a common synthetic colorant, promotes experimental colitis via intestinal serotonin in gut microbiota-dependent and -independent pathways in mice.[14] SY was prioritized due to its widespread usage and insufficient toxicological characterization in inflammatory bowel contexts.

Sunset yellow (SY), a common azo dye, is approved for use as a food additive in many countries, though it has been banned in Finland and Norway. In 2009, the European Food Safety Authority (EFSA) reassessed SY's safety as a food additive with the European Union, temporarily reducing its acceptable daily intake (ADI) to 1 mg/kg bw/day. Following re-evaluation, EFSA established an updated ADI of SY 4 mg/kg bw/day.[15] Even at the ADI level, SY has been shown to negatively impact brain tissue by inducing oxidative stress.[16] SY exhibited teratogenic effects on chicken embryos, causing hepatocyte necrosis and multiple degenerative changes in the kidney.[17] Additionally, research has shown that SY can induce colitis in mice through dysregulated IL-23 expression.[18] SY has also been observed to alter the gut microbiota of male Wistar rats, compromising intestinal integrity.[19] However, the effect of SY on colitis has not been clearly elucidated.

Received: May 20, 2025
Revised: August 22, 2025
Accepted: August 25, 2025
Published: September 3, 2025

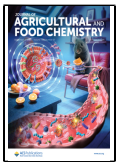

In this study, the effects and underlying mechanism of SY on the pathogenesis of colitis were investigated by integrating gut microbiota sequencing profiling, metabolomics, and fecal microbiota transplantation (FMT). Long-term exposure to SY increased susceptibility to experimental colitis in mice, accompanied by altered gut microbiota and serum metabolic profiles. Notably, FMT from SY-exposed mice also exacerbated DSS-induced colitis, revealing the critical role of gut microbiota. Additionally, SY exposure aggravated DSS-induced oxidative stress by disrupting glutathione (GSH) metabolism. Furthermore, SY exposure impaired the sulfur metabolism of *AKK*, which may have contributed to its reduced abundance both in vitro and in vivo. GSH supplementation markedly reversed the SY-induced inhibition of *AKK* growth. These findings indicated that chronic exposure to SY promotes experimental colitis by altering GSH metabolism in a gut microbiota-dependent manner. This study highlights the need for stricter evaluation of SY usage in the food industry and may enhance public awareness of potential health risks associated with dietary colorants.

MATERIALS AND METHODS

Animals. Male C57BL/6J mice, aged 5−6 weeks, were purchased from the Animal Core Facility of Nanjing Medical University. All mice were housed in a specific pathogen-free (SPF) chamber with free access to autoclaved standard food and water. The environmental conditions were controlled at 50−53% humidity and a temperature of 21−22 °C, with a 12 h light/dark cycle. Before any experiments were begun, the mice were acclimated for 7 days. In this study, mice (n = 10 per group) were exposed to SY ($C_{16}H_{10}N_2Na_2O_7S_2$, CAS: 2783-94-0, Sigma-Aldrich, USA) in drinking water (0.1% w/v, 0.1 mg/mL) for 13 weeks. The dose of the SY level was chosen based on the EFSA revised maximum allowable level in food. During this procedure, water was changed twice a week, and the intake of SY was about 0.4 mg/day per mouse. A human equivalent dose of 1.3 mg/kg/day was calculated from the FDA guidelines for scaling between species,[20] which did not reach the ADI of SY 4 mg/kg bw/day. Experimental colitis was induced by 2% DSS (molecular mass 36−50 kDa, MP Biomedicals, USA) for 7 days (from weeks 12 to 13). All animal experiments were approved by the Institutional Animal Care and Use Committee (IACUC) of Nanjing Medical University (IACUC-2302039).

Depletion of Gut Microbiota. The mice were orally gavaged with 200 μL cocktail of antibiotics (ABX) for 1 week to deplete gut microbiota. The ABX contains 50 mg/kg/day vancomycin hydrochloride (Maclin Biochemical Technology Co., Ltd., Shanghai, China), 1 mg/kg/day amphitromycin B, 100 mg/kg/day neomycin sulfate (Solarbio Science & Technology Co., Ltd., Beijing, China), 100 mg/kg/day metronidazole, and 100 mg/kg/day, ambenomycin sodium (Sangon Biotech Co., Ltd., Shanghai, China).

Fecal Microbiota Transplantation. Following 12 weeks of treatment with either 0.1 mg/mL SY or water (control), fresh fecal samples were collected from the donor mice. Then, 10 mg aliquots of feces were homogenized in 1 mL of sterile PBS. The suspensions were then centrifuged at 600 × g for 5 min at room temperature to pellet insoluble particulate matter. All sample processing was performed immediately after collection to ensure sample integrity.[21] Recipient mice (n = 10 per group) were treated with ABX for 1 week to deplete gut microbiota, and then they were orally administered with 200 μL suspension once every 3 days for 3 weeks. Then, these mice were given 2% DSS for 1 week and then changed to normal drinking water for 1 day to recover.

Assessment of Colitis Severity. Disease activity index (DAI) is a combined score of weight loss, stool viscosity, and fecal bleeding. The scoring method was as follows: weight loss: 0 = no loss, 1 = 0−5%, 2 = 5−10%, 3 = 10−20%, 4 > 20%; stool: 0 = normal, 2 = soft stool, 4 = loose stool; and bleeding: 0 = no blood, 2 = a little blood, 3 = distinct blood, and 4 = gross blood (blood around anus). Scores were conducted during DSS treatment.

Hematoxylin and Eosin and Immunohistochemical (IHC) Staining. The colon was washed with normal saline, fixed with 4% paraformaldehyde for 24 h, embedded with paraffin, and stained with hematoxylin and eosin (H&E). After air drying for a week, all colon tissue sections were observed and analyzed using a Pannoramic digital section scanner (Pannoramic SCAN, 3DHISTECH Kft, Budapest, Hungary). Pathological scores were evaluated blindly according to previously published methods.[22] Briefly, the slices were scored based on three parameters of tissue damage and four parameters of inflammation, and these scores were multiplied with factors that considered how affected the tissue was.

For IHC staining, 5 mm-thick paraffin-embedded sections were deparaffinized. Different sets of colon sections were used for IHC staining to assess the expression of Muc2 and ZO-1. Staining intensity was evaluated by using ImageJ software.

Quantitative Real-Time Polymerase Chain Reaction. Total RNA from colon tissues was extracted using Trizol reagent (Tiangen Biotech, Beijing) and quantified using NanoDrop 2000 (Thermo Fisher Scientific, Canada). Complementary DNA (cDNA) was prepared from 1 μg of total RNA using HiScript II Q RT SuperMix (Vazyme Biotech, Nanjing, China). Relative quantitative real-time polymerase chain reaction (qRT-PCR) amplification was performed using LightCycler 480 II (Roche, Ltd.) with specific primers. Data were analyzed according to the $2^{-\Delta\Delta CT}$ method with *GAPDH* as the internal standard. Primer sequences are listed in Table S1.

Enzyme-Linked Immunosorbent Assay (ELISA). Colon tissue was homogenized in PBS (pH 7.4, 0.01 M) supplemented with protease inhibitor. The colon homogenates were then centrifuged at 5000 × g for 10 min at 4 °C, and the supernatant was stored at 80 °C until analysis. The levels of colonic IL-1β and TNF-α were measured by ELISA per manufacturer's procedure (Elabscience, Wuhan, China).

Western Blotting. Protein extraction from colonic tissues was performed using the Protein Extraction Kit (KeyGEN biotech, KGB5303-50), with protein concentrations quantified using the BCA Protein Assay Reagent (Beyotime Biotechnology, Shanghai, China). Protein samples were denatured by boiling at 95 °C for 5 min in Laemmli buffer, separated by 10% SDS-PAGE, and subsequently transferred to polyvinylidene difluoride membranes (Millipore, Billerica, MA, USA). Membranes were blocked and then incubated overnight at 4 °C with rabbit anti-Occludin (1:1000, Proteintech, 27260-1-AP), rabbit anti-ZO-1 (1:5000, Proteintech, 21773-1-AP) or mouse anti-GAPDH (1:1000, Proteintech, 10494-1-AP). Following primary antibody incubation, membranes were probed with the appropriate horseradish peroxidase (HRP)-conjugated secondary antibodies. Protein bands were visualized using an enhanced chemiluminescence detection system, and band intensities were quantified using ImageJ software.

16S rRNA Sequencing. Total DNA was extracted from the collected stool samples. The quality, concentration, and purity of DNA were detected by 1% agarose gel electrophoresis and instruments. 27F (5′-AGAGTTTGATCCTGGCTCAG-3′) and 1492R (5′-GGTTACCTTGTTACGACTT-3′) were used to amplify the full-length 16S rRNA gene. The PCR products were recovered, purified, and quantified. The quantitative PCR products were sequenced by an Illumina MiSeq instrument (PE300). Operational taxonomic unit (OTU) clustering was performed based on the optimized sequences to obtain OTU tables. Subsequently, the data were analyzed on the Majorbio online platform (www.majorbio.com). Among them, the gut microbiota health index (GMHI) was calculated using a biologically interpretable mathematical formula for predicting the likelihood of disease independent of the clinical diagnosis. GMHI is more robust and consistent predictor of disease presence (or absence) compared to α-diversity indices.[23] Microbiota dysbiosis index (MDI) was calculated as the log of (total abundance in genera increased in the disease group) over (total abundance in genera decreased in the disease group).[24] Phylogenetic Investigation of Communities by Reconstruction of Unobserved States 2 (PICRUSt2)

https://doi.org/10.1021/acs.jafc.5c06410
J. Agric. Food Chem. 2025, 73, 23633−23643

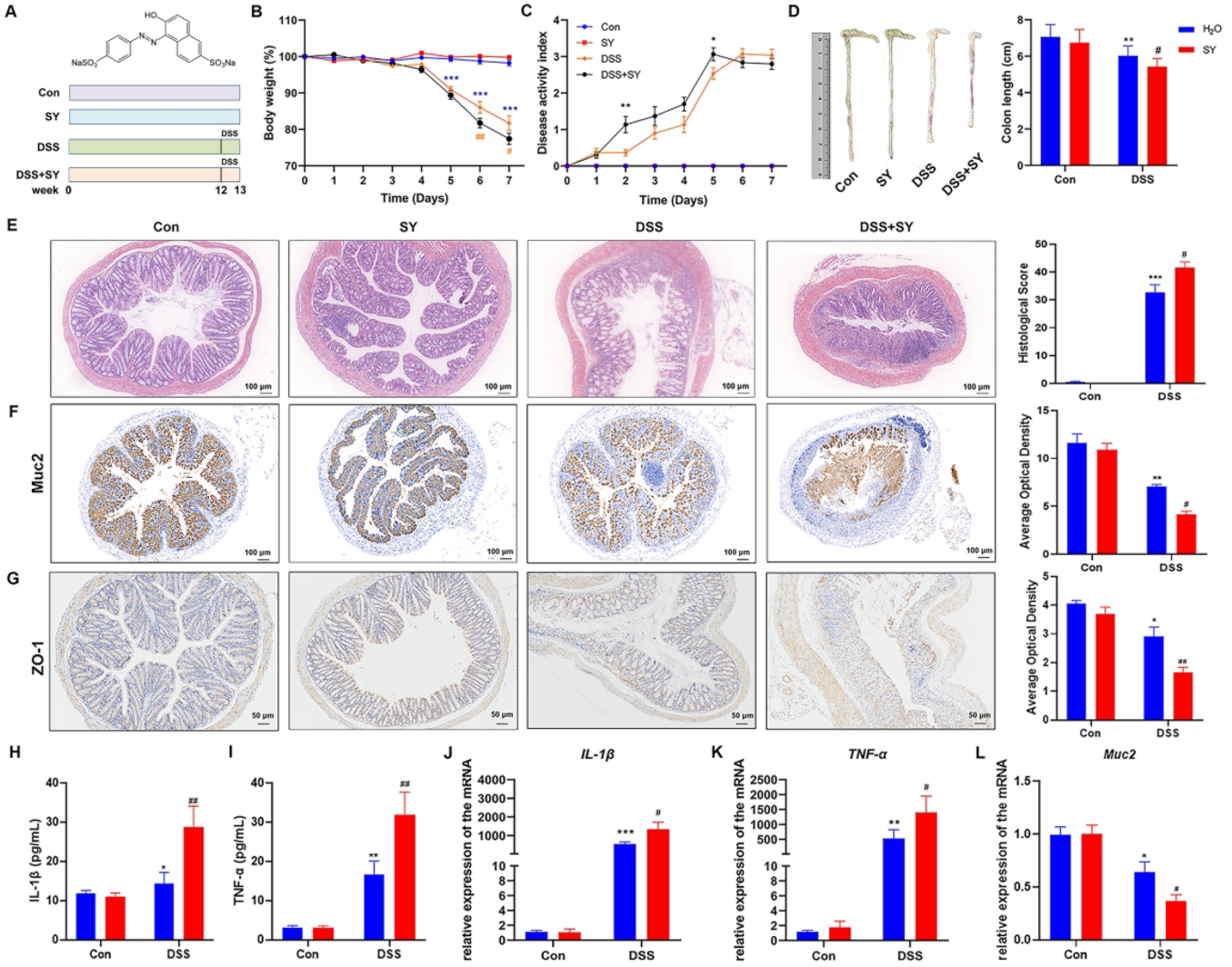

Figure 1. SY exposure increased susceptibility to colitis. (A) Schematic diagram of the experimental design (n = 10). (B) Body weight is expressed as the mean change from the starting body weight. (C) Disease activity index (DAI). (D) Colon length. (E) Representative HE staining of colon and pathological scores (n = 5), scale bar: 100 μm. IHC staining and average optical density of (F) Muc2 and (G) ZO-1 in distal colon sections, scale bar: 100 μm (n = 5). The levels of (H) IL-1β and (I) TNF-α expression in the colon tissues. The mRNA expression of (J) *IL-1β*, (K) *TNF-α*, and (L) *MUC-2* in the colon tissues (n = 10). Data were presented as the mean ± SEM and analyzed by ordinary two-way ANOVA with Tukey's multiple comparisons. *P < 0.05, **P < 0.01, ***P < 0.001 compared with the control group; #P < 0.05, ##P < 0.01 compared with the intragroup.

was used to predict the functional information on microbial communities, and Kyoto Encyclopedia of Genes and Genomes (KEGG) combined with STAMP software (version 2.1.3) was used to analyze the species and functional composition and differences.

Serum Metabolomes and Data Processing. The UHPLC Ultimate 3000 system coupled with a Q Exactive hybrid quadrupole-orbitrap mass spectrometer (UPLC-MS) was employed to analyze serum metabolic profiling according to our previous study.[25] An aliquot of the same volume from each sample were pooled to prepare the quality control (QC) sample for checking the stability of the instrument. Simca14.0 software (version 14.1.0.2047) was used for systematic analysis, such as orthogonal partial least-squares discriminant analysis (OPLS-DA), to obtain variable weight importance ranking (VIP). The statistically differential metabolites were identified according to VIP > 1, P value < 0.05, and fold change > 1.2. The metabolic pathways were annotated using MetaboAnalyst 6.0 (www.metaboanalyst.ca) and the KEGG database.

Bacterium Culture. *AKK* MucT (ATCC BAA-835) was cultured in brain heart infusion broth supplemented with 10 mg/L resazurin (an oxidation−reduction indicator) and 0.1 mg/L cysteine under strict anaerobic conditions.[26] Five concentration gradients of SY were introduced into the anaerobic culture tube in accordance with the Chinese national standards for use of food additives of China (GB 2760−2024). To explore the role of oxidative stress in *AKK* growth, *AKK* was treated with 1.0 mg/L SY in the presence or absence of 1 M GSH for 24 h. The growth of *AKK* was monitored by using a bacterial turbidimeter.

Measurement of Oxidative Stress. *AKK* was treated with 1.0 mg/L SY for 24 h and harvested for homogenization in PBS to extract the total protein. Following centrifugation at 12,000 rpm for 15 min at 4 °C, the supernatant was collected for protein quantification using a BCA protein assay kit. Then, reactive oxygen species (ROS) levels, GSH contents, and GST activity were determined in accordance with the manufacturer's protocols (Jiancheng Bioengineering Institute, Nanjing, China).

Prokaryotic Transcriptome Analysis. *AKK* was treated with or without 1 mg/mL SY for 24 h, after which the bacteria were collected for RNA extraction. The TruSeq Stranded Total RNA Library Prep kit (Illumina, CA, USA) was used to prepare the sequence library. Library sequencing was performed on an Illumina HiSeq4000 SBS instrument (CA, USA). Differential expression analysis was conducted using EdgeR, with differentially expressed genes identified based on the criteria of FDR < 0.05 and |log2FC| ≥ 1. Functional enrichment of

https://doi.org/10.1021/acs.jafc.5c06410
J. Agric. Food Chem. 2025, 73, 23633−23643

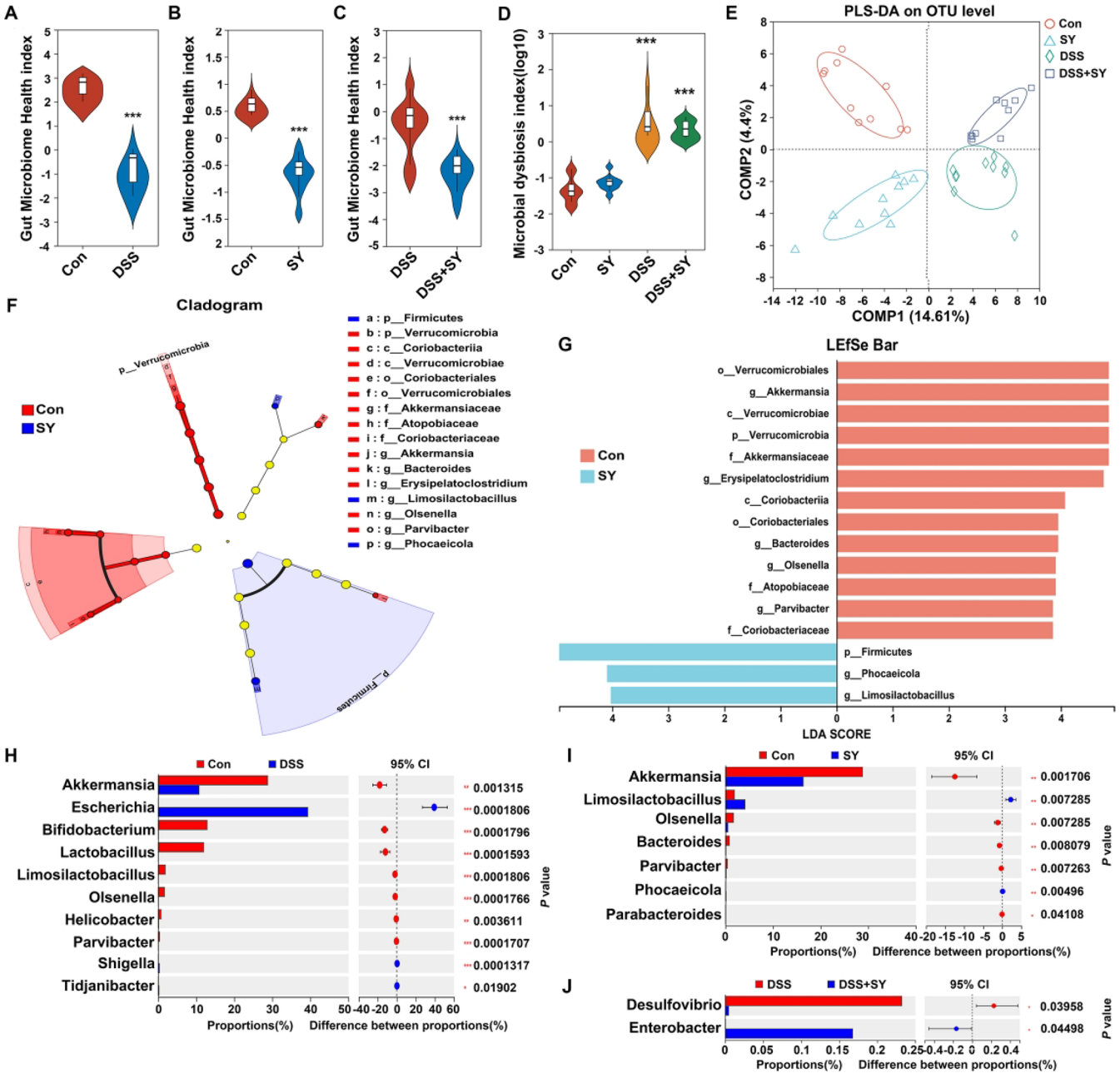

Figure 2. Alterations in the composition and function of gut microbiota induced by SY exposure. Gut microbiota health index in normal mice followed by (A) DSS and (B) SY treatment (n = 10). (C) Gut microbiota health index of colitis mice exposed to SY. (D) Microbial dysbiosis index among the four groups. (E) Projection to latent structure discriminant analysis (PLS-DA) of the OTU among groups. (F) Cladogram based on LEfSe analysis was used to show the community composition of the gut microbiota. (G) Differentially enriched gut microbiota in each group at the genus level by linear discriminant analysis (LDA). (H) Differential bacteria at the genus level between control and DSS groups. Differential bacteria at the genus level in (I) normal and (J) colitis mice exposed to SY. Data were presented as the mean ± SEM and analyzed by the Wilcoxon rank-sum test. ***P < 0.001 compared with the control group.

KEGG pathways and Gene Ontology (GO) terms was subsequently performed using the Majorbio online platform.

Statistical Analysis. The data of body weight, DAI, colon length, and gene expression were analyzed using a two-tailed t test or ANOVA with Tukey's multiple comparisons. The Wilcoxon rank-sum test was used to compare the difference in bacteria between the two groups. Correlations between metagenomics and metabolomics data were analyzed using the Mantel test and Spearman's rank test. All data are presented as mean ± SEM unless otherwise stated. P < 0.05 was considered statistically significant.

RESULTS

SY Exposure Aggravated DSS-Induced Colitis in Mice.

To investigate the effect of SY on the development of colitis, C57BL/6 mice were given drinking water with or without SY (0.1 mg/mL) throughout the experiment, followed by treatment with 2% DSS in the last week (Figure 1A). Mice treated with DSS experienced weight loss (P < 0.001), which was further exacerbated in the SY-exposed group (P < 0.001, Figure 1B). Mice in the SY+DSS group exhibited a higher DAI (P < 0.01) and significantly reduced colon length (P < 0.05)

https://doi.org/10.1021/acs.jafc.5c06410
J. Agric. Food Chem. 2025, 73, 23633−23643

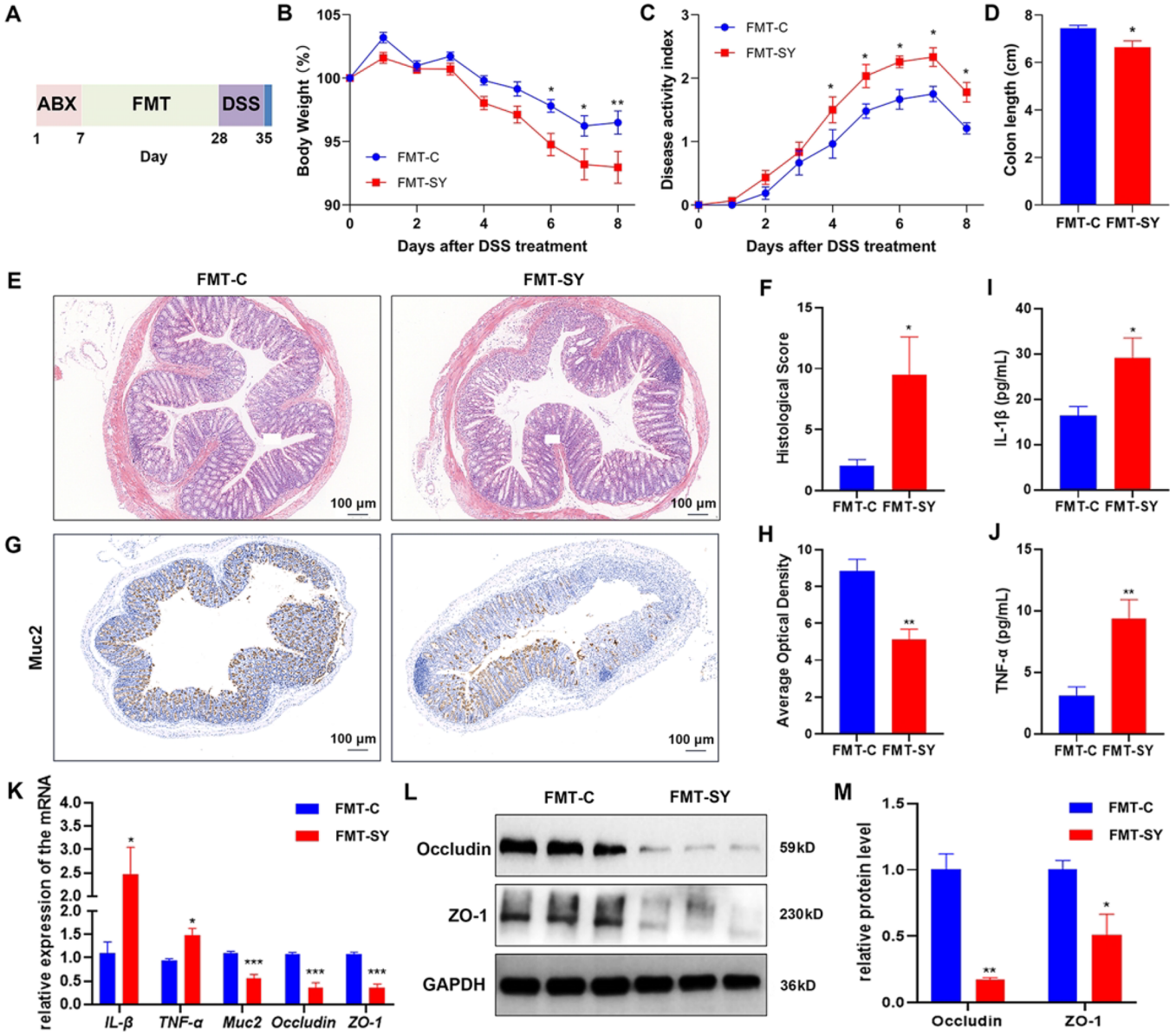

Figure 3. Gut microbiota-mediated exacerbation of colitis in SY-treated mice. (A) Schematic diagram of the experimental design (n = 10). (B) Body weight. Data for weight changes from the starting body weight. (C) Disease activity index. (D) Colon length. (E) Representative HE staining of colon and (F) pathological scores (n = 5), scale bar: 100 μm. (G) IHC staining for Muc2 in distal colon sections and (H) average optical density, scale bar: 100 μm. The levels of (I) IL-1β and (J) TNF-α in the colon tissues. (K) The mRNA expression of *IL-1β*, *TNF-α*, *MUC-2*, *Occludin*, and *ZO-1* in the colon tissues. (L) Representative image of Western blot and (M) relative quantification of Occludin, ZO-1, and GAPDH. Data were presented as the mean ± SEM and analyzed by an unpaired two-tailed t test. *P < 0.05, **P < 0.01, ***P < 0.001, compared with the control group.

compared to the DSS-only group (Figure 1C,D). Histological analysis revealed greater destruction of crypt structures and extensive infiltration of immune cells in the mucosa and submucosa, and an elevated pathological score in the SY+DSS group in comparison with the DSS group (P < 0.05, Figure 1E). Furthermore, SY exposure significantly inhibited the expression of Muc2 and ZO-1 in DSS-induced colitis mice, exacerbating the impairment of the intestinal mucus barrier (P < 0.05, Figure 1F,G). Colonic IL-1β and TNF-α levels were significantly increased in the DSS+SY group (P < 0.01, Figure 1H,I). Additionally, the expression of IL-1β and TNF-α was higher in the DSS+SY group compared to the DSS group (P < 0.05, Figure 1J,K). Meanwhile, the expression of *Muc2* was decreased in the DSS+SY group (P < 0.05, Figure 1L).

SY Altered Gut Microbiota Composition and Decreased the Abundance of *AKK*. Next, we investigated whether the gut microbiota contributed to the increased susceptibility to colitis in SY-exposed C57BL/6 mice. Compared to the control (Con) group, the GMHI was significantly decreased (P < 0.001) in both the DSS group (Figure 2A) and the SY group (Figure 2B), with a further reduction (P < 0.001) observed in the DSS+SY (Figure 2C). Additionally, the MDI increased (P < 0.001) in both the DSS and DSS+SY groups (Figure 2D). These findings suggest that the intestinal health of mice with UC was negatively impacted by exposure to SY. Despite significant interindividual variation, partial least squares discriminant analysis (PLS-DA) revealed distinct clustering of fecal microbiota among the four groups

https://doi.org/10.1021/acs.jafc.5c06410
J. Agric. Food Chem. 2025, 73, 23633−23643

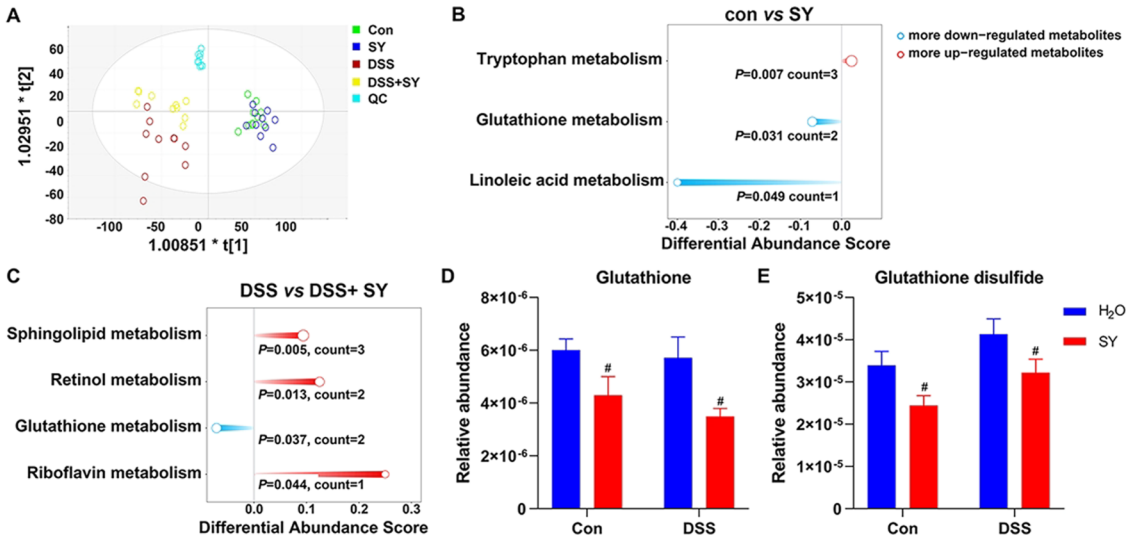

Figure 4. SY exposure disrupted glutathione metabolism. (A) PLS-DA plots of serum metabolomics among groups (n = 10). (B) Pathway analysis of differential metabolites in normal mice with or without SY exposure. (C) Pathway analysis of differential metabolites in colitis mice with or without SY exposure. The relative intensity of serum (D) glutathione and (E) glutathione disulfide. Data were presented as the mean ± SEM and analyzed by ordinary two-way ANOVA with Tukey's multiple comparisons and unpaired two-tailed t test, #P < 0.05, compared with the intragroup.

(Figure 2E), indicating group-specific differences in gut microbial composition. The microbial cladogram of differential abundance and linear discriminant analysis effect size (LEfSe) analysis revealed that SY had a significant impact on Verrucomicrobia (phylum level), Akkermansiaceae (family level), and *Akkermansia* (genus level) (Figure 2F,G). Notably, the relative abundance of *AKK* in both the SY and DSS groups was significantly lower than that in the control group (Figure 2H,I). The proportion of *Enterobacter* in the DSS+SY group was higher than that in the DSS group (Figure 2J).

Gut Microbiota Mediated the Exacerbation of Colitis in Mice Exposed to SY. Alterations in microbiota composition and metabolism have been shown to regulate susceptibility to colitis. Thus, we hypothesized that the SY-induced shift in gut microbiota composition and activity predisposed SY-treated mice to colitis. To test the role of the gut microbiota, the impact of FMT was assessed (Figure 3A). Mice that received fecal transplants from SY-exposed mice (FMT-SY) showed increased colitis severity compared to those that received feces from control mice (FMT-C), as evidenced by significant weight loss (P < 0.05), higher DAI scores (P < 0.05), and shorter colon length (P < 0.05) in the FMT-SY group (Figure 3B−D). Histological analysis revealed inflammatory cell infiltration, destruction of crypt structures, and elevated pathological score in the FMT-SY group (P < 0.05, Figure 3E,F). IHC staining revealed a significant reduction in Muc2 expression compared to the FMT-C group (P < 0.01, Figure 3G,H). The levels of IL-1β (P < 0.05) and TNF-α (P < 0.01) in the colon tissues from the FMT-SY group were significantly increased compared with those from the FMT-C group (Figure 3I,J). Colonic mRNA expression of *IL-1β* and *TNF-α* was upregulated in the FMT-SY group, while *Muc2*, *Occludin*, and *ZO-1* were significantly downregulated compared with the FMT-C group (P < 0.001, Figure 3K). Moreover, the protein expression of Occludin and ZO-1 was downregulated in the FMT-SY group, revealing impairment of the gut barrier (Figure 3L,M).

SY Exposure Disrupted the GSH Metabolism. We conducted serum metabolomics to investigate how exposure to SY affects the relevant molecular mechanisms. PLS-DA analysis revealed significant differences in the serum metabolic profiles of mice treated with or without DSS (Figure 4A). Notably, SY-exposed mice exhibited enrichment in the GSH metabolism pathway, irrespective of whether they were treated with DSS (Figure 4C) or not (Figure 4B). Both GSH and glutathione disulfide (GSSG) levels were significantly downregulated (P < 0.05) across groups (Figure 4D,E).

SY Exposure Regulated GSH-Related Genes and Gut Microbiota Function. The expression of glutathione peroxidase (*GSH-Px*), *GST*, catalase (*CAT*), and cyclooxygenase-2 (*COX2*) in colon tissue was markedly decreased following SY exposure (P < 0.05, Figure 5A−D). Additionally, we observed significant reductions in the mRNA levels of *GSH-Px*, *GST*, *CAT*, and *COX2* in the colon tissues of FMT-SY mice (P < 0.05, Figure 5E−H). The Mantel test was performed to assess the relationship between SY-associated genera and differential metabolites between the control and SY groups. The relative abundance of *AKK* was positively correlated with GSH levels (Figure 5I). Additionally, PICRUSt2 analysis indicated that exposure to SY significantly inhibited the sulfur metabolism of gut microbiota in mice treated with or without DSS (P < 0.001, Figure 5J). These data suggested that SY exposure disrupted GSH metabolism by regulating the host's related genes and modulation of gut microbiota.

SY Inhibited the Growth of *AKK* by Disrupting GSH Metabolism. Bacteria were cultured *in vitro* to further elucidate the effects of SY on *AKK*. A dose-dependent decrease in *AKK* viability (P < 0.05) was observed following exposure to varying doses of SY (Figure 6A). SY exposure significantly increased ROS levels (P < 0.001, Figure 6B), decreased GSH contents, and suppressed GST activity (P < 0.05, Figure 6C,D) in *AKK*. RNA-seq analysis was performed to gain further insight into the potential mechanisms linked to the effect of *AKK* on GSH metabolism. *AKK* followed SY treatment had a total of 64 differentially expressed genes (DEGs), of which 19 were upregulated and 45 were downregulated (Figure 6E). Among them, the expression of *phosphoadenylyl-sulfate (PAPS)*

https://doi.org/10.1021/acs.jafc.5c06410
J. Agric. Food Chem. 2025, 73, 23633−23643

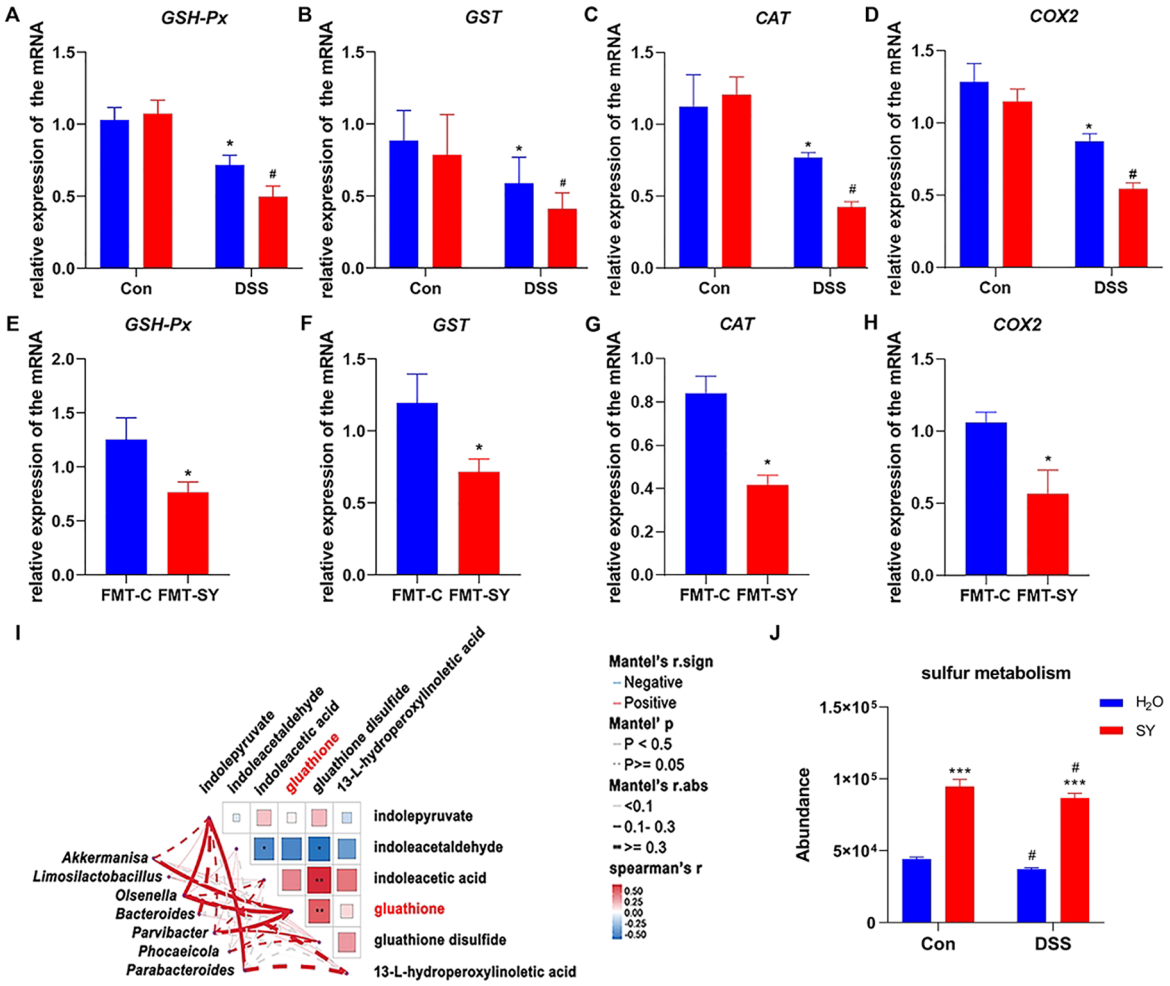

Figure 5. SY exposure GSH-related genes and gut microbiota function. (A–D) Colonic mRNA expression of *GSH-px*, *GST*, *CAT*, and *COX2* in mice chronically exposed to SY (n = 10). (E–H) Colonic mRNA expression of *GSH-px*, *GST*, *CAT*, and *COX2* in mice treated with fecal bacteria transplants (n = 10). (I) Mantel test of differential genera with metabolites in the glutathione metabolism pathway between Con and SY groups. (J) The abundance of sulfur metabolism predicted by PICRUSt 2.0 (n = 10). Data were presented as the mean ± SEM and analyzed by unpaired two-tailed t test and ordinary two-way ANOVA with Tukey's multiple comparisons. *P < 0.05, ***P < 0.001, compared with the control group; #P < 0.05, compared with the intragroup.

reductase, cysteine kinase (*CysK*), and cysteine synthase (*CysD*) was downregulated (Figure 6F). Gene Ontology (GO) enrichment analysis revealed that the DEGs were primarily associated with sulfur- and sulfate-related biological processes (Figure 6G). Sulfur metabolism was the most enriched pathway in response to the SY treatment (Figure 6H). Notably, GSH supplementation effectively restored *AKK* growth inhibited by SY (P < 0.001, Figure 6I).

DISCUSSION

Since the 19th century, shifts in diet and lifestyle have led to an increase in the consumption of processed foods, which coincided with the rise of IBD. By the late 20th century, both the incidence and prevalence of IBD had significantly increased.[27] Humans are exposed to various chemicals daily through their diet, and children's diets, in particular, are rich in synthetic pigments that enhance the visual appeal of foods. While the dietary risk factors linked to chronic disease have been identified,[28−30] our understanding of the role of food colorants in the pathogenesis of IBD remains limited. In this study, we provide evidence that the widely used synthetic colorant SY enhances susceptibility to colitis in mice under healthy conditions by altering the gut microbiota composition and function.

Although the exact cause of IBD remains unknown, disruption in gut microbiota composition and function are recognized as key factors that increase susceptibility to IBD.[31,32] This study demonstrated that SY exacerbated DSS-induced colon inflammation and gut microbiota dysbiosis, as evidenced by reduced GMHI and increased MDI. FMT is an efficacious tool for repairing the gut microbiota. Germ mice receiving an FMT from obese mice treated with aspartame or stevia, a low-calorie sweetener, had greater weight gain and body fat and impaired glucose tolerance compared with control mice.[33] Thus, we validated the role of gut microbiota in SY-trigged UC by FMT experiment. Mice receiving FMT from SY-exposed mice exhibited worsened DSS-induced colitis, indicating that gut microbiota mediated this exacerbation, corroborating recent findings on food additive-microbiota interactions.[34,35] Consistent with previous studies,[36,37] we observed a significant increase in the abundance of *Escherichia* and *Shigella* at the genus level in mice with DSS-induced colitis. Additionally, SY increased the relative abundance of *Enterobacter* at the genus level, which was overabundant in

https://doi.org/10.1021/acs.jafc.5c06410
J. Agric. Food Chem. 2025, 73, 23633−23643

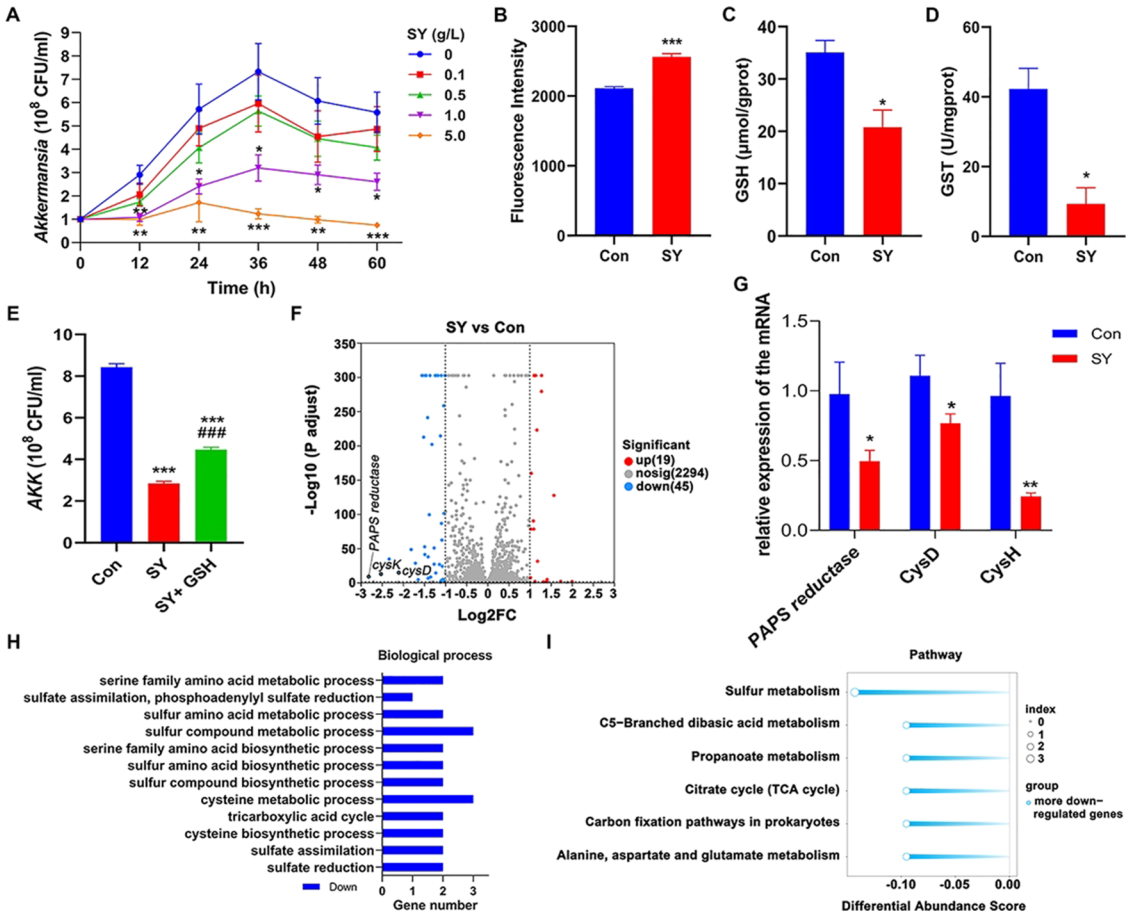

Figure 6. SY-inhibited *AKK* growth by disrupting GSH metabolism. (A) Inhibitory effects of SY on *AKK* growth (B) ROS levels, (C) GSH contents, and (D) GST activity in *AKK* following SY exposure ($n = 5$). (E) GSH-mediated restoration of SY-inhibited *AKK* growth. (F) Numbers of differentially expressed genes (DEGs). (G) mRNA expression of phosphoadenylyl-sulfate reductase, CysK, and CysD in *AKK*. (H) Altered GO terms and (I) pathway analysis of DEGs in biological process. Data were presented as the mean ± SEM and analyzed by ordinary two-way ANOVA with Tukey's multiple comparisons and unpaired two-tailed *t* test. *$P < 0.05$, **$P < 0.01$, ***$P < 0.001$, compared with the control group; ###$P < 0.001$, compared with the intragroup.

patients with colorectal cancer (CRC).[38] Notably, the significant depletion of *AKK* observed in our study parallels the dysbiotic effects reported for common food additives.[39,40] Both DSS and SY exposure reduced the relative abundance of *AKK*, a beneficial microbe that colonizes the intestinal mucus layer and has been identified as a promising target for IBD treatment.[41,42] These findings indicated that gut microbiota mediated the exacerbation of DSS-induced colitis by SY in mice.

The metabolomics approach provides substantial evidence of altered metabolic profiles and disrupted metabolic pathways in patients with IBD.[43,44] In line with a previous study,[45] mice with DSS-colitis also exhibited a distinct metabolic profile compared to the control group. SY exposure disrupted three metabolic pathways under normal conditions and four pathways under colitis conditions, with GSH metabolism being the overlapping pathway. GSH metabolism plays a crucial role in cellular redox reactions, providing antioxidant defenses and regulating physiological processes in both humans and other organisms.[46,47] Our findings revealed that serum concentrations of both GSH and GSSG were significantly decreased in mice exposed to SY. As the most abundant intracellular antioxidant, GSH neutralizes ROS and limits their accumulation.[48] Within cells, GSH levels are dynamically maintained by GSH reductase, which regenerates GSH from GSSG during redox cycling, while antioxidant enzymes, such as GSH-Px and glutaredoxin, facilitate GSSG production during oxidative detoxification.[49]

High levels of ROS can cause cell damage during oxidative stress and are closely associated with the pathological process of UC.[50] When GSH metabolism is disrupted, insufficient GSH fails to adequately defend against ROS damage, leading to an imbalance in intestinal homeostasis.[51,52] To counteract ROS-mediated tissue damage, endogenous defense mechanisms employ antioxidant enzymes, such as GSH-Px, Gst, CAT, and COX2.[53] Food additives are generally recognized as safe, and SY did not show any kind of mutagenic and carcinogenic effects. A few studies also documented that it even exhibited antioxidant and anti-inflammatory properties.[54] However, SY exposure exacerbated the upregulation of these genes, especially in colitis mice, indicating that SY may enhance oxidative-stress-mediated colonic damage. This selective modulation warrants further investigation into the safety of food additives under subhealth and even pathological conditions.

AKK is positively associated with intestinal and metabolic health,[55] and *AKK* treatment has been proven to ameliorate high-fat and high-cholesterol diet-induced oxidative stress, thereby inhibiting apoptosis in gut.[56] *AKK* ameliorated the intestinal mucosal damage caused by cadmium through

https://doi.org/10.1021/acs.jafc.5c06410
J. Agric. Food Chem. 2025, 73, 23633−23643

increasing melatonin production and scavenging ROS.[57] SY exposure inhibited the growth of *AKK* both in vivo and in vitro. The relative abundances of *AKK* and serum GSH were positively correlated following SY exposure. Our results were further supported by studies showing that oral administration of *AKK* caused significant changes in GSH metabolism and increased GSH concentration in mice by spatially resolved metabolomics analysis.[58] SY disrupted the sulfur metabolism of gut microbiota, especially in *AKK*.

SY exposure may significantly decrease the contents of GSH and downregulate the expression of *PAPS reductase*, *CysK*, and *CysD*, involved in sulfur metabolism in *AKK*. These findings suggest impaired sulfur assimilation, which may directly impact GSH biosynthesis since cysteine availability serves as the primary rate-limiting factor.[59] Notably, GSH supplementation significantly reversed the SY-induced inhibition of *AKK* growth. These findings indicate that SY may inhibit *AKK* growth by triggering oxidative stress through the disruption of sulfur metabolism.

This study is the first to demonstrate that long-term exposure to SY increases the susceptibility to DSS-induced colitis. The adverse health effects of SY were mediated by gut microbiota disruption, specifically evidenced by reduced abundance of *AKK* and altered sulfur metabolism. SY exacerbated intestinal inflammation through a GSH metabolism disruption. However, several shortcomings remain. The dose used may not fully represent the average human exposure in daily life, suggesting the need for population-based studies, including those of patients with IBD, to determine if synthetic food coloring intake correlates with colitis development. Given that dietary products often contain multiple colorants, it would also be valuable to investigate whether interactions among these additives influence colitis susceptibility. As research on the link between gut microbiota dysbiosis and IBD progresses, diet is increasingly recognized as a public health concern. Our findings lay a foundation for exploring the role of SY in colitis and open avenues for examining the impact of other food colorants on IBD pathogenesis.

■ ASSOCIATED CONTENT

Supporting Information

The Supporting Information is available free of charge at https://pubs.acs.org/doi/10.1021/acs.jafc.5c06410.

Table S1: the primers sequences used for PCR reaction (PDF)

Accession Codes

The 16S rRNA sequencing data from mice feces (GSA: CRA031881) and RNA sequencing data of *AKK* (GSA: CRA019778) had been submitted to Genome Sequence Read Archive, National Genomics Data Center, China that publicly accessible.

■ AUTHOR INFORMATION

Corresponding Author

Zhan Zhang − *Department of Health Inspection and Quarantine, School of Public Health, Key Laboratory of Public Health Safety and Emergency Prevention and Control Technology of Higher Education Institutions in Jiangsu Province and Key Lab of Modern Toxicology of Ministry of Education, School of Public Health, Nanjing Medical University, Nanjing 211166, P.R. China;* orcid.org/0000-0002-9685-5753; Phone: +86-25-8686-8401; Email: zhanzhang@njmu.edu.cn; Fax: +86-25-8686-8499

Authors

Xinyi Shi − *Department of Health Inspection and Quarantine, School of Public Health, Key Laboratory of Public Health Safety and Emergency Prevention and Control Technology of Higher Education Institutions in Jiangsu Province and Key Lab of Modern Toxicology of Ministry of Education, School of Public Health, Nanjing Medical University, Nanjing 211166, P.R. China*

Li Wan − *Department of Health Inspection and Quarantine, School of Public Health, Key Laboratory of Public Health Safety and Emergency Prevention and Control Technology of Higher Education Institutions in Jiangsu Province and Key Lab of Modern Toxicology of Ministry of Education, School of Public Health, Nanjing Medical University, Nanjing 211166, P.R. China*

Shanhong Ni − *Department of Health Inspection and Quarantine, School of Public Health, Key Laboratory of Public Health Safety and Emergency Prevention and Control Technology of Higher Education Institutions in Jiangsu Province and Key Lab of Modern Toxicology of Ministry of Education, School of Public Health, Nanjing Medical University, Nanjing 211166, P.R. China*

Xin Wu − *Department of Health Inspection and Quarantine, School of Public Health, Key Laboratory of Public Health Safety and Emergency Prevention and Control Technology of Higher Education Institutions in Jiangsu Province and Key Lab of Modern Toxicology of Ministry of Education, School of Public Health, Nanjing Medical University, Nanjing 211166, P.R. China*

Jing Mu − *Department of Health Inspection and Quarantine, School of Public Health, Key Laboratory of Public Health Safety and Emergency Prevention and Control Technology of Higher Education Institutions in Jiangsu Province and Key Lab of Modern Toxicology of Ministry of Education, School of Public Health, Nanjing Medical University, Nanjing 211166, P.R. China*

Wenlong Pei − *Department of Health Inspection and Quarantine, School of Public Health, Key Laboratory of Public Health Safety and Emergency Prevention and Control Technology of Higher Education Institutions in Jiangsu Province and Key Lab of Modern Toxicology of Ministry of Education, School of Public Health, Nanjing Medical University, Nanjing 211166, P.R. China*

Zeyuan Chen − *Department of Health Inspection and Quarantine, School of Public Health, Key Laboratory of Public Health Safety and Emergency Prevention and Control Technology of Higher Education Institutions in Jiangsu Province, Nanjing Medical University, Nanjing 211166, P.R. China*

Yu Xia − *Department of Health Inspection and Quarantine, School of Public Health, Key Laboratory of Public Health Safety and Emergency Prevention and Control Technology of Higher Education Institutions in Jiangsu Province, Nanjing Medical University, Nanjing 211166, P.R. China; Department of Laboratory Science, Suzhou Center for Disease Control and Prevention, Suzhou 215131, P.R. China*

Lei Li − *Department of Health Inspection and Quarantine, School of Public Health, Key Laboratory of Public Health Safety and Emergency Prevention and Control Technology of Higher Education Institutions in Jiangsu Province and Key*

Lab of Modern Toxicology of Ministry of Education, School of Public Health, Nanjing Medical University, Nanjing 211166, P.R. China; orcid.org/0000-0003-1836-186X

Complete contact information is available at: https://pubs.acs.org/10.1021/acs.jafc.5c06410

Author Contributions

Z.Z. and L.L. conceived, designed, and supervised the project; X.Y.S., L.L., and L.W. performed all animal experiments and RT-qPCR analysis; S.H.N., X.W., and J.M. performed metabonomics and glutathione metabolites analysis; W.L.P., Z.Y.C., and Y.X. performed 16S rRNA-seq and RNA-seq analysis. X.Y.S., Z.Z., and L.L. organized all figures; X.Y.S. wrote the manuscript; Z.Z. revised the manuscript; all authors validated and approved the final manuscript. X.Y.S. and L.W. contributed equally.

Funding

This work was supported by National Natural Science Foundation of China (No. 82373627), and Postgraduate Research & Practice Innovation Program of Jiangsu Province (SJCX24_0808).

Notes

The authors declare no competing financial interest.

REFERENCES

(1) Le Berre, C.; Honap, S.; Peyrin-Biroulet, L. Ulcerative colitis. *Lancet* **2023**, *402* (10401), 571−584.

(2) Heller, C.; Moss, A. C.; Rubin, D. T. Overview to Challenges in IBD 2024−2029. *Inflamm. Bowel Dis.* **2024**, *30* (Supplement_2), S1−S4.

(3) Kontola, K.; Oksanen, P.; Huhtala, H.; Jussila, A. Increasing Incidence of Inflammatory Bowel Disease, with Greatest Change Among the Elderly: A Nationwide Study in Finland, 2000−2020. *J. Crohns Colitis* **2023**, *17* (5), 706−711.

(4) Kobayashi, T.; Siegmund, B.; Le Berre, C.; Wei, S. C.; Ferrante, M.; Shen, B.; Bernstein, C. N.; Danese, S.; Peyrin-Biroulet, L.; Hibi, T. Ulcerative colitis. *Nat. Rev. Dis Primers* **2020**, *6* (1), 74.

(5) Gros, B.; Kaplan, G. G. Ulcerative Colitis in Adults: A Review. *JAMA* **2023**, *330* (10), 951−965.

(6) Glassner, K. L.; Abraham, B. P.; Quigley, E. M. M. The microbiome and inflammatory bowel disease. *J. Allergy Clin Immunol* **2020**, *145* (1), 16−27.

(7) Adolph, T. E.; Zhang, J. Diet fuelling inflammatory bowel diseases: preclinical and clinical concepts. *Gut* **2022**, *71* (12), 2574−2586.

(8) Mentella, M. C.; Scaldaferri, F.; Pizzoferrato, M.; Gasbarrini, A.; Miggiano, G. A. D. Nutrition, IBD and Gut Microbiota: A Review. *Nutrients* **2020**, *12* (4), 944.

(9) Gonza, I.; Goya-Jorge, E.; Douny, C.; Boutaleb, S.; Taminiau, B.; Daube, G.; Scippo, M. L.; Louis, E.; Delcenserie, V. Food additives impair gut microbiota from healthy individuals and IBD patients in a colonic in vitro fermentation model. *Food Res. Int.* **2024**, *182*, No. 114157.

(10) Um, C. Y.; Hodge, R. A.; Tran, H. Q.; Campbell, P. T.; Gewirtz, A. T.; McCullough, M. L. Association of Emulsifier and Highly Processed Food Intake with Circulating Markers of Intestinal Permeability and Inflammation in the Cancer Prevention Study-3 Diet Assessment Sub-Study. *Nutr Cancer* **2022**, *74* (5), 1701−1711.

(11) Whelan, K.; Bancil, A. S.; Lindsay, J. O.; Chassaing, B. Ultra-processed foods and food additives in gut health and disease. *Nat. Rev. Gastroenterol Hepatol* **2024**, *21* (6), 406−427.

(12) Elmore, S. E.; Cano-Sancho, G.; La Merrill, M. A. Disruption of normal adipocyte development and function by methyl- and propyl-paraben exposure. *Toxicol. Lett.* **2020**, *334*, 27−35.

(13) Ruiz, P. A.; Moron, B.; Becker, H. M.; Lang, S.; Atrott, K.; Spalinger, M. R.; Scharl, M.; Wojtal, K. A.; Fischbeck-Terhalle, A.; Frey-Wagner, I.; et al. Titanium dioxide nanoparticles exacerbate DSS-induced colitis: role of the NLRP3 inflammasome. *Gut* **2017**, *66* (7), 1216−1224.

(14) Kwon, Y. H.; Banskota, S.; Wang, H.; Rossi, L.; Grondin, J. A.; Syed, S. A.; Yousefi, Y.; Schertzer, J. D.; Morrison, K. M.; Wade, M. G.; et al. Chronic exposure to synthetic food colorant Allura Red AC promotes susceptibility to experimental colitis via intestinal serotonin in mice. *Nat. Commun.* **2022**, *13* (1), 7617.

(15) Hazards, E. P. o. B.; Koutsoumanis, K.; Allende, A.; Alvarez-Ordonez, A.; Bolton, D.; Bover-Cid, S.; Chemaly, M.; De Cesare, A.; Hilbert, F.; Lindqvist, R.; et al. Update of the list of qualified presumption of safety (QPS) recommended microbiological agents intentionally added to food or feed as notified to EFSA 20: Suitability of taxonomic units notified to EFSA until March 2024. *EFSA J.* **2024**, *22* (7), No. e8882.

(16) Bhatt, D.; Vyas, K.; Singh, S.; John, P. J.; Soni, I. P. Sunset Yellow induced biochemical and histopathological alterations in rat brain sub-regions. *Acta Histochem* **2024**, *126* (3), No. 152155.

(17) Colakoglu, F.; Selcuk, M. L. The Embryotoxic Effects of in Ovo Administered Sunset Yellow FCF in Chick Embryos. *Vet Sci.* **2021**, *8* (2), 31.

(18) He, Z.; Chen, L.; Catalan-Dibene, J.; Bongers, G.; Faith, J. J.; Suebsuwong, C.; DeVita, R. J.; Shen, Z.; Fox, J. G.; Lafaille, J. J.; et al. Food colorants metabolized by commensal bacteria promote colitis in mice with dysregulated expression of interleukin-23. *Cell Metab.* **2021**, *33* (7), 1358−1371.

(19) Zahran, S. A.; Mansour, S. M.; Ali, A. E.; Kamal, S. M.; Romling, U.; El-Abhar, H. S.; Ali-Tammam, M. Sunset Yellow dye effects on gut microbiota, intestinal integrity, and the induction of inflammasomopathy with pyroptotic signaling in male Wistar rats. *Food Chem. Toxicol.* **2024**, *187*, No. 114585.

(20) Nair, A. B.; Jacob, S. A simple practice guide for dose conversion between animals and human. *J. Basic Clin Pharm.* **2016**, *7* (2), 27−31.

(21) Yao, X.; Zhang, C.; Xing, Y.; Xue, G.; Zhang, Q.; Pan, F.; Wu, G.; Hu, Y.; Guo, Q.; Lu, A.; et al. Remodelling of the gut microbiota by hyperactive NLRP3 induces regulatory T cells to maintain homeostasis. *Nat. Commun.* **2017**, *8* (1), 1896.

(22) Tortora, S. C.; Bodiwala, V. M.; Quinn, A.; Martello, L. A.; Vignesh, S. Microbiome and colorectal carcinogenesis: Linked mechanisms and racial differences. *World J. Gastrointest Oncol* **2022**, *14* (2), 375−395.

(23) Gupta, V. K.; Kim, M.; Bakshi, U.; Cunningham, K. Y.; Davis, J. M., 3rd; Lazaridis, K. N.; Nelson, H.; Chia, N.; Sung, J. A predictive index for health status using species-level gut microbiome profiling. *Nat. Commun.* **2020**, *11* (1), 4635.

(24) Gunathilake, M.; Lee, J.; Choi, I. J.; Kim, Y. I.; Yoon, J.; Sul, W. J.; Kim, J. F.; Kim, J. Alterations in Gastric Microbial Communities Are Associated with Risk of Gastric Cancer in a Korean Population: A Case-Control Study. *Cancers* **2020**, *12* (9), 2619.

(25) Ren, Y.; Shi, X.; Mu, J.; Liu, S.; Qian, X.; Pei, W.; Ni, S.; Zhang, Z.; Li, L.; Zhang, Z. Chronic exposure to parabens promotes non-alcoholic fatty liver disease in association with the changes of the gut microbiota and lipid metabolism. *Food Funct* **2024**, *15* (3), 1562−1574.

(26) Liu, S.; Zhao, S.; Cheng, Z.; Ren, Y.; Shi, X.; Mu, J.; Ge, X.; Dai, Y.; Li, L.; Zhang, Z. Akkermansia muciniphila Protects Against Antibiotic-Associated Diarrhea in Mice. *Probiotics Antimicrob Proteins* **2024**, *16* (4), 1190−1204.

(27) Lewis, J. D.; Parlett, L. E.; Jonsson Funk, M. L.; Brensinger, C.; Pate, V.; Wu, Q.; Dawwas, G. K.; Weiss, A.; Constant, B. D.; McCauley, M.; et al. Incidence, Prevalence, and Racial and Ethnic Distribution of Inflammatory Bowel Disease in the United States. *Gastroenterology* **2023**, *165* (5), 1197−1205.

(28) Amchova, P.; Siska, F.; Ruda-Kucerova, J. Food Safety and Health Concerns of Synthetic Food Colors: An Update. *Toxics* **2024**, *12* (7), 466.

(29) Zhang, Q.; Chumanevich, A. A.; Nguyen, I.; Chumanevich, A. A.; Sartawi, N.; Hogan, J.; Khazan, M.; Harris, Q.; Massey, B.;

Chatzistamou, I.; et al. The synthetic food dye, Red 40, causes DNA damage, causes colonic inflammation, and impacts the microbiome in mice. *Toxicol Rep* **2023**, *11*, 221−232.
(30) Karimi, F.; Khodabandeh, Z.; Nazari, F.; Dara, M.; Masjedi, F.; Momeni-Moghaddam, M. Post-Weaning Exposure to Sunset Yellow FCF Induces Changes in Testicular Tight and Gap Junctions in Rats: Protective Effects of Coenzyme Q10. *Reprod Sci.* **2023**, *30* (10), 2962−2972.
(31) Haneishi, Y.; Furuya, Y.; Hasegawa, M.; Picarelli, A.; Rossi, M.; Miyamoto, J. Inflammatory Bowel Diseases and Gut Microbiota. *Int. J. Mol. Sci.* **2023**, *24* (4), 3817.
(32) Foppa, C.; Rizkala, T.; Repici, A.; Hassan, C.; Spinelli, A. Microbiota and IBD: Current knowledge and future perspectives. *Dig Liver Dis* **2024**, *56* (6), 911−922.
(33) Nettleton, J. E.; Cho, N. A.; Klancic, T.; Nicolucci, A. C.; Shearer, J.; Borgland, S. L.; Johnston, L. A.; Ramay, H. R.; Noye Tuplin, E.; Chleilat, F.; et al. Maternal low-dose aspartame and stevia consumption with an obesogenic diet alters metabolism, gut microbiota and mesolimbic reward system in rat dams and their offspring. *Gut* **2020**, *69* (10), 1807−1817.
(34) Ulcerative colitis. *Nat. Rev. Dis Primers* **2020**, *6* (1), 73. DOI: .
(35) Guo, M.; Liu, X.; Tan, Y.; Kang, F.; Zhu, X.; Fan, X.; Wang, C.; Wang, R.; Liu, Y.; Qin, X.; et al. Sucralose enhances the susceptibility to dextran sulfate sodium (DSS) induced colitis in mice with changes in gut microbiota. *Food Funct* **2021**, *12* (19), 9380−9390.
(36) Yao, S.; Zhao, Z.; Wang, W.; Liu, X. Bifidobacterium Longum: Protection against Inflammatory Bowel Disease. *J. Immunol. Res.* **2021**, *2021*, No. 8030297.
(37) Aghamohammad, S.; Sepehr, A.; Miri, S. T.; Najafi, S.; Pourshafie, M. R.; Rohani, M. Anti-inflammatory and immunomodulatory effects of Lactobacillus spp. as a preservative and therapeutic agent for IBD control. *Immun Inflamm Dis* **2022**, *10* (6), No. e635.
(38) Masi, A. C.; Embleton, N. D.; Lamb, C. A.; Young, G.; Granger, C. L.; Najera, J.; Smith, D. P.; Hoffman, K. L.; Petrosino, J. F.; Bode, L.; et al. Human milk oligosaccharide DSLNT and gut microbiome in preterm infants predicts necrotising enterocolitis. *Gut* **2021**, *70* (12), 2273−2282.
(39) Liu, X.; Zhang, B.; Zhang, Y.; Li, W.; Yin, J.; Shi, A.; Wang, J.; Wang, S. 2'-Fucosyllactose Promotes Colonization of Akkermansia muciniphila and Prevents Colitis In Vitro and in Mice. *J. Agric. Food Chem.* **2024**, *72* (9), 4765−4776.
(40) Daniel, N.; Gewirtz, A. T.; Chassaing, B. Akkermansia muciniphila counteracts the deleterious effects of dietary emulsifiers on microbiota and host metabolism. *Gut* **2023**, *72* (5), 906−917.
(41) Bae, M.; Cassilly, C. D.; Liu, X.; Park, S. M.; Tusi, B. K.; Chen, X.; Kwon, J.; Filipcik, P.; Bolze, A. S.; Liu, Z.; et al. Akkermansia muciniphila phospholipid induces homeostatic immune responses. *Nature* **2022**, *608* (7921), 168−173.
(42) Zheng, M.; Han, R.; Yuan, Y.; Xing, Y.; Zhang, W.; Sun, Z.; Liu, Y.; Li, J.; Mao, T. The role of Akkermansia muciniphila in inflammatory bowel disease: Current knowledge and perspectives. *Front Immunol* **2023**, *13*, 1089600.
(43) Vich Vila, A.; Zhang, J.; Liu, M.; Faber, K. N.; Weersma, R. K. Untargeted faecal metabolomics for the discovery of biomarkers and treatment targets for inflammatory bowel diseases. *Gut* **2024**, *73* (11), 1909−1920.
(44) Wang, J.; Sun, Q.; Gao, Y.; Xiang, H.; Zhang, C.; Ding, P.; Wu, T.; Ji, G. Metabolomics window into the diagnosis and treatment of inflammatory bowel disease in recent 5 years. *Int. Immunopharmacol.* **2022**, *113* (Pt B), No. 109472.
(45) Gu, Z.; Pei, W.; Shen, Y.; Wang, L.; Zhu, J.; Zhang, Y.; Fan, S.; Wu, Q.; Li, L.; Zhang, Z. Akkermansia muciniphila and its outer protein Amuc_1100 regulates tryptophan metabolism in colitis. *Food Funct* **2021**, *12* (20), 10184−10195.
(46) Li, B.; Guo, Y.; Jia, X.; Cai, Y.; Zhang, Y.; Yang, Q. Luteolin alleviates ulcerative colitis in rats via regulating immune response, oxidative stress, and metabolic profiling. *Open Med. (Wars)* **2023**, *18* (1), 20230785.
(47) Koch, R. L.; Stanton, J. B.; McClatchy, S.; Churchill, G. A.; Craig, S. W.; Williams, D. N.; Johns, M. E.; Chase, K. R.; Thiesfeldt, D. L.; Flynt, J. C.; et al. Discovery of genomic loci for liver health and steatosis reveals overlap with glutathione redox genetics. *Redox Biol.* **2024**, *75*, No. 103248.
(48) Bonetti, L.; Horkova, V.; Grusdat, M.; Longworth, J.; Guerra, L.; Kurniawan, H.; Franchina, D. G.; Soriano-Baguet, L.; Binsfeld, C.; Verschueren, C.; et al. A Th17 cell-intrinsic glutathione/mitochondrial-IL-22 axis protects against intestinal inflammation. *Cell Metab.* **2024**, *36* (8), 1726−1744.
(49) Wang, L.; Ahn, Y. J.; Asmis, R. Sexual dimorphism in glutathione metabolism and glutathione-dependent responses. *Redox Biol.* **2020**, *31*, No. 101410.
(50) Yan, X.; Meng, L.; Zhang, X.; Deng, Z.; Gao, B.; Zhang, Y.; Yang, M.; Ma, Y.; Zhang, Y.; Tu, K.; et al. Reactive oxygen species-responsive nanocarrier ameliorates murine colitis by intervening colonic innate and adaptive immune responses. *Mol. Ther* **2023**, *31* (5), 1383−1401.
(51) Guo, W.; Li, K.; Sun, B.; Xu, D.; Tong, L.; Yin, H.; Liao, Y.; Song, H.; Wang, T.; Jing, B.; et al. Dysregulated Glutamate Transporter SLC1A1 Propels Cystine Uptake via Xc(−) for Glutathione Synthesis in Lung Cancer. *Cancer Res.* **2021**, *81* (3), 552−566.
(52) Ocansey, D. K. W.; Yuan, J.; Wei, Z.; Mao, F.; Zhang, Z. Role of ferroptosis in the pathogenesis and as a therapeutic target of inflammatory bowel disease (Review). *Int. J. Mol. Med.* **2023**, *51* (6), 56.
(53) El-Akabawy, G.; El-Sherif, N. M. Zeaxanthin exerts protective effects on acetic acid-induced colitis in rats via modulation of pro-inflammatory cytokines and oxidative stress. *Biomed Pharmacother* **2019**, *111*, 841−851.
(54) Singh, S.; Yadav, S.; Cavallo, C.; Mourya, D.; Singh, I.; Kumar, V.; Shukla, S.; Shukla, P.; Chaudhary, R.; Maurya, G. P.; et al. Sunset Yellow protects against oxidative damage and exhibits chemoprevention in chemically induced skin cancer model. *NPJ. Syst. Biol. Appl.* **2024**, *10* (1), 23.
(55) Zhao, Q.; Yu, J.; Hao, Y.; Zhou, H.; Hu, Y.; Zhang, C.; Zheng, H.; Wang, X.; Zeng, F.; Hu, J.; et al. Akkermansia muciniphila plays critical roles in host health. *Crit Rev. Microbiol* **2023**, *49* (1), 82−100.
(56) Rao, Y.; Kuang, Z.; Li, C.; Guo, S.; Xu, Y.; Zhao, D.; Hu, Y.; Song, B.; Jiang, Z.; Ge, Z.; et al. Gut Akkermansia muciniphila ameliorates metabolic dysfunction-associated fatty liver disease by regulating the metabolism of L-aspartate via gut-liver axis. *Gut Microbes* **2021**, *13* (1), 1−19.
(57) Xie, S.; Zhang, R.; Li, Z.; Liu, C.; Xiang, W.; Lu, Q.; Chen, Y.; Yu, Q. Indispensable role of melatonin, a scavenger of reactive oxygen species (ROS), in the protective effect of Akkermansia muciniphila in cadmium-induced intestinal mucosal damage. *Free Radic. Biol. Med.* **2022**, *193* (Pt 1), 447−458.
(58) Zhu, Z.; Cai, J.; Hou, W.; Xu, K.; Wu, X.; Song, Y.; Bai, C.; Mo, Y. Y.; Zhang, Z. Microbiome and spatially resolved metabolomics analysis reveal the anticancer role of gut Akkermansia muciniphila by crosstalk with intratumoral microbiota and reprogramming tumoral metabolism in mice. *Gut Microbes* **2023**, *15* (1), 2166700.
(59) Cassier-Chauvat, C.; Marceau, F.; Farci, S.; Ouchane, S.; Chauvat, F. The Glutathione System: A Journey from Cyanobacteria to Higher Eukaryotes. *Antioxidants* **2023**, *12* (6), 1199.

https://doi.org/10.1021/acs.jafc.5c06410
J. Agric. Food Chem. 2025, 73, 23633−23643